Detection of Small Horizontal Defects in Thin Isotropic Plates Using Ultrasonic Rayleigh-Lamb Waves

M. D. Gilchrist
Mechanical Engineering Department, University College Dublin, Belfield, Dublin 4, Ireland
eMail: Michael.Gilchrist@ucd.ie

ABSTRACT

This paper considers the detection of symmetric crack-like defects in thin metallic plates using longitudinal ultrasonic waves. Only physically small defect sizes are considered in order that the initial stages of crack growth, for example during fatigue, can be detected. This method has the potential to be significantly faster for non-destructively detecting defects than conventional ultrasonic techniques, which rely on transverse waves propagating through the thickness of a plate. It is shown, using analytical and computational methods, that it is possible to obtain measurable reflection coefficients due to the attenuation of a longitudinal ultrasonic wave by physically small defects.

KEYWORDS

Non-destructive testing, Rayleigh-Lamb wave, crack, ultrasonics

NOMENCLATURE

a	=	half crack length
c	=	speed of S_0 wave
c_l	=	speed of longitudinal wave in an infinite medium
c_t	=	speed of transverse wave in an infinite medium
d	=	half thickness of plate (= 0.5mm)
k	=	wave number ($= 2\pi/\lambda$)
u, v	=	in-plane and normal displacements, respectively
x, y	=	Cartesian co-ordinates
λ	=	wavelength
λ_1, μ_1	=	Lamé constants ($= 55.6E9 kg/m/s^2$, $26.4E9 kg/m/s^2$, respectively)
ν	=	Poisson ratio (= 0.34)
ρ	=	density of plate ($= 2700 kg/m^3$)
E	=	Young's modulus (= 70.7GPa)
ω	=	angular frequency ($= 2\pi$. frequency)
Ω	=	nondimensional frequency
	=	π . plate thickness . frequency / c_t ($= \omega d/c_t$)

1 INTRODUCTION

It is becoming increasingly important to be able to assess rapidly the integrity of engineering structures which are being used for increasingly longer service lives and in safety-critical applications. This is particularly relevant for high-performance materials such as polymer-, metal- and ceramic-matrix composites, and many of the high-modulus and high-strength metallic alloys that are used in aerospace, automotive, pressure vessel and pipeline industries. For many of these applications it is necessary to identify the initial stages of crack propagation, originating perhaps from some void or inclusion, as early as possibly since the rate at which a crack will subsequently develop can accelerate quickly and lead to catastrophic failure of the structure.

Conventional non-destructive evaluation (NDE) by ultrasonic C-scanning, for example, uses high frequency waves (of the order of MHz) which propagate transversely through the thickness of a plate. A single transducer can be used both to emit incident waves into a plate and to receive reflected waves whilst a double transducer system will have a receiving transducer located on the opposite side of the plate from the emitting transducer. Such systems can characterise the position and dimensions of a defect with good accuracy. However, to assess an area of plate requires that the transducer(s) scans the complete surface; this is particularly time consuming for large plates. The method proposed in this paper is for longitudinal waves, rather than transverse waves, to be propagated along the length of a plate and to monitor the attenuation of such a wave. Because guided waves (i.e., Rayleigh-Lamb waves) travel large distances without attenuation (in a non-lossy material) they are ideally suited for NDE of large structures and components that are difficult to inspect. It is not expected that this procedure will identify a defect as accurately as conventional transverse waves, although it should provide some estimate of the position of a defect in a plate. The primary advantage of this procedure is that the need to scan the surface of a plate is avoided and consequently, the time required to assess the integrity of a plate is reduced by at least an order of magnitude. Should this method identify the presence of a defect above some critical size, conventional transverse ultrasonic waves could subsequently be used to characterise the defect more accurately.

A wide range of physical defects can exist in metallic and composite material systems, and many engineering fractures tend to initiate at the site of naturally-occurring material imperfections such as voids, inclusions and crack-like defects. Within metals such defects could be porosities, impurities, imperfections, slag, etc., while delaminations, matrix cracks, fibre fracture and splitting can often be the source of failure of composite systems. Defects such as delaminations along ply interfaces in composites, impurities along the rolling direction of hot- or cold-rolled metals, or surface machining scratches are orientated in particular directions. Other defects can be unevenly aligned and randomly distributed throughout a material. Many such defects are often microscopically small and will propagate due to applied forces, for example, in-flight loads on a rotorcraft, or internal pressure in a filament-wound composite pressure vessel. It is only when a defects has grown to a certain size that it will be detected by means of some NDE technique. At that stage, maintenance scheduling is used to monitor the development and growth rate of defects before they reach the critical size at which catastrophic failure of the structure will occur.

The scattering of Rayleigh-Lamb waves by an anisotropic weldment in a metal plate has been analysed by Datta and co-workers [Al-Nasser et al., 1991] using a hybrid finite element method. These results showed that maximum sensitivity during NDE (reflection coefficients of up to 70%) could be achieved by operating in certain frequency ranges ($3 < \Omega < 8$) and by probing with certain modes (symmetric S_0 mode). The same method has also been used to predict reflection coefficients associated with S_0 (symmetric) and A_0 (antisymmetric) waves scattered by transverse cracks in laminated composite plates [Datta et al., 1988, 1990; Bratton et al., 1991; Karunasena et al., 1991a, b; Ju & Datta, 1992]. However, the main disadvantages of this hybrid method is that it is limited to sub megahertz frequencies and that it is not immediately compatible with commercially available finite element software.

Guo & Cawley [1993] showed that the amplitude of the reflection of the S_0 Rayleigh-Lamb wave from a delamination in a composite plate is strongly dependent upon the position of the delamination through the thickness of the laminate. The delamination locations corresponding to the maximum and minimum reflectivity correspond to the locations of maximum and minimum shear stress across the interface in the S_0 mode. Delaminations of 10- to 20-mm diameter (= O(wavelength) in size) were detected at a range of up to 500mm in 8-ply laminates [Guo & Cawley, 1993]. However, delaminations could not be detected at interfaces through the thickness of a composite laminate that were free of shear stress.

Rokhlin [1979] has similarly examined delaminations in rolled sheets where the length of the delaminations was greater than the wavelength of the Rayleigh-Lamb waves. Negligible reflection coefficients were predicted using an analytical method. The most promising method for long-range inspection [Guo & Cawley, 1994] was a pulse-echo configuration in which the S_0 mode is generated by a transmitting transducer and reflections of the same mode are monitored returning to a receiver placed close to the transmitter.

A simple example of an aligned defect, which is amenable to mathematical analysis, is that of a two-dimensional horizontal crack, symmetrically embedded in a large metal sheet (infinite thin plate). This paper will consider the scattering and attenuation of longitudinal waves by such a crack, oriented parallel to the plane of a sheet, as identified in Fig. 1. It is physically small defect sizes (<1mm in length) that are considered in order that the initial stages of crack propagation may be detected. A combined analytical and computational method is used to predict the reflection coefficients of Rayleigh-Lamb waves by such defects.

The scattering of low frequency (large wavelength) waves by wedge-shaped internal and surface cracks in plates has also been analysed by Koshiba et al. [1984]. The reflection coefficient of the internal crack was shown to be highly dependent upon the wedge apex angle although this was not the case for the surface crack. However, Koshiba's work is limited to a single frequency, whereas the present paper is applicable to a range of frequencies. Like Koshiba et al., this paper is restricted to cracks which are symmetric about the central plane of the plate.

2 THEORETICAL ANALYSIS

For an S wave, the general formulae for the complex displacements in the *x*, y directions, namely, *u*, v, are given [Viktorov, 1967] by

$$u = +ik\left[\frac{\cosh qy}{\sinh qd} - \frac{2qs}{k^2+s^2}\cdot\frac{\cosh sy}{\sinh sd}\right]e^{i(kx-\omega t)} \tag{1}$$

$$v = +q\left[\frac{\sinh qy}{\sinh qd} - \frac{2k^2}{k^2+s^2}\cdot\frac{\sinh sy}{\sinh sd}\right]e^{i(kx-\omega t)} \tag{2}$$

where

$$q = \sqrt{k^2 - k_l^2} \quad \text{and} \quad s = \sqrt{k^2 - k_t^2} \tag{3}$$

and

$$k = 2\pi/\lambda \qquad k_l/k = c/c_l \qquad k_t/k = c/c_t \tag{4}$$

The displacement of the surface *y=0* is given by

$$u(y=0) = ik\left[\frac{1}{s_1} - \frac{2qs}{k^2+s^2}\cdot\frac{1}{s_2}\right]e^{i(kx-\omega t)} \tag{5}$$

$$s_1 = \sinh qd, \qquad s_2 = \sinh sd$$

The formula for the normal stress, τ_{yy}, is given by

$$\tau_{yy} = \lambda_1\left[\frac{\partial u}{\partial x} + \frac{\partial v}{\partial y}\right] + 2\mu_1\frac{\partial v}{\partial y} \tag{6}$$

Restricting this analysis to a Poisson ratio ν=1/3, which is reasonably close to that of aluminium. In this case

$$\lambda_1 = 2\mu_1 \qquad c_l = 2c_t \tag{7}$$

Now c, k are connected by the dispersion relation for S waves. When ν=1/3 this relation may be written in the form

$$\tan u = \frac{4\sqrt{\left(1-\frac{\bar{c}^2}{4}\right)\left(\bar{c}^2-1\right)}}{\left(2-\bar{c}^2\right)^2}\tanh\left[u\sqrt{\frac{1-\frac{\bar{c}^2}{4}}{\bar{c}^2-1}}\right] \tag{8}$$

where

$$\begin{aligned}\bar{c} &= c/c_t \\ \bar{k} &= kd \\ u &= \bar{k}\sqrt{\bar{c}^2-1}\end{aligned} \tag{9}$$

The value of u corresponding to a particular value of $\bar{c}$ can be obtained by a process of iteration. Thus, the value of u corresponding to a fixed $\bar{c}$ is estimated and substituted into the right side of Eq. (8). This provides an estimate for tan$u$ and hence a better approximation to u. This value of u is then substituted into the right side of Eq. (8) and a more accurate value of tan$u$ is obtained. A few iterations suffice to give an accurate value of u corresponding to a given value of $\bar{c}$. The value of $\bar{k}$ can then be found using the 3rd relation of Eq. (9). Finally, the value of Ω corresponding to $\bar{c}$ can be obtained using the result

$$\Omega = \bar{c}\bar{k} \tag{10}$$

Table 1 gives values of $\bar{k}$ corresponding to typical values of Ω. From this table values of k and c, and therefore q, s, s_1 and s_2 can be calculated and hence the values of the stress τ_{yy}.

Ω	kd	λ/d	c/c_t
0.534	0.31	20.3	1.72
1.0	0.59	10.6	1.70
1.6	0.97	6.47	1.64

Table 1. Relationship between wave frequency, wave number, wavelength and wave speed in thin aluminium plate.

Eq. (7) for the normal stress reduces to

$$\tau_{yy} = 2\mu_1\left[\frac{\partial u}{\partial x} + 2\frac{\partial v}{\partial y}\right]$$

Calculating the out of plane stress on the plane $y=0$ gives that

$$\left(\frac{\partial u}{\partial x}\right)_{y=0} = -k^2\left[\frac{1}{s_1} - \frac{2qs}{k^2+s^2}\cdot\frac{1}{s_2}\right]e^{i(kx-\omega t)}$$

$$2\left(\frac{\partial v}{\partial y}\right)_{y=0} = 2q\left[\frac{q}{s_1} - \frac{2k^2 s}{k^2+s^2}\cdot\frac{1}{s_2}\right]e^{i(kx-\omega t)}$$

$$\left|\frac{\tau_{yy}}{2\mu_1}\right| = \frac{1}{s_1}\left[-k^2+2q^2\right] + \frac{1}{s_2}\left[\frac{2qsk^2}{k^2+s^2} - \frac{4qsk^2}{k^2+s^2}\right]$$

$$= \frac{1}{s_1}\left[-k^2+2q^2\right] + \frac{1}{s_2}\left[-\frac{2qsk^2}{k^2+s^2}\right]$$

$$= \frac{1}{s_1}\left[-k^2+2k^2-2k_l^2\right] + \frac{1}{s_2}\left[-\frac{2qsk^2}{k^2+s^2}\right]$$

$$= \frac{1}{s_1}\left[k^2-2k_l^2\right] - \frac{1}{s_2}\left[\frac{2qsk^2}{k^2+s^2}\right]$$

where the amplitude of an S_0 wave, which produces a pressure of 1Pa on the crack face, is given by $|u_{(y=0)}|/|\tau_{yy}|$ [Crane et al., 1997]. Three different frequencies have been considered and the corresponding amplitudes of incident S_0 waves have been calculated and are given in Table 2.

Ω	incident wave amplitude [m]
0.534	49.44E-14
1.000	12.54E-14
1.600	2.308E-14

Table 2. Amplitudes of in-plane displacements of incident S_0 waves.

The reflection coefficients associated with the defects in the various cracked plates are calculated as the ratio of the amplitude of the reflected wave to that of the incident wave. Specifically, the amplitudes of the reflected waves are calculated computationally by modelling the propagation of a sinusoidal wave, of pressure 1Pa, as described below in Section 3.

3 COMPUTATIONAL ANALYSIS

A series of two-dimensional finite element models of cracked plates were created using commercial software [ABAQUS, 1996]. Because the cracks are all symmetrically located within the plates there are two planes of symmetry and it has only been necessary to model one quarter of each plate. Figure 2 details the model of the cracked plate a/d = 0.6; finite element models for the other analyses were of similar construction. The same plate dimensions have been assumed in all the numerical analyses: a half-thickness of 0.5mm and a half-length of 130.0mm. Such a large ratio of plate length to thickness is necessary to ensure that the wavelength of the high frequency waves is a small fraction of the plate length.

All finite element models were meshed with regular plane strain isoparametric quadrilateral elements with only vertex nodes and 3x3 integration points. Eight elements were used to model the plate half-thickness which provided 24 Gaussian integration points to represent the model variables through the 0.5mm plate half-thickness. Ten elements were used to model the half-length of the crack and 520 for the remaining uncracked half-length of the

plate. Consequently, each model consisted of 4240 elements. The boundary conditions appropriate to the various planes of symmetry and the cracked region of the plates were enforced and material properties were specified for aluminium (Young's modulus = 70.7GPa, Poisson ratio = 0.34, density = 2700.0kg/m^3). Model symmetry within the various cracked plates was defined by restraining the vertical (y-axis) displacements of nodes on the y=0 plane and by restraining the in-plane (x-axis) displacements of uncracked nodes on the x=0 plane. Merely by changing the material properties of elements within the model to those of steel, or indeed another metallic material, would have provided a finite element model of a crack in a different plate. However, since the initial application for this work is primarily aimed at light-weight high performance engineering structures, it is only aluminium that has been modelled. Subsequent research will perform similar investigations for fibre reinforced polymer matrix composites.

A dynamic sinusoidal load, of amplitude $|P_n|$ and angular frequency ω, identical to that of the incident wave, was applied normally outwards from the plane of the crack to simulate the propagation of the reflected wave. The sinusoidal reflected wave for the case Ω=1 was defined by

$$P_n = \cos(\omega t)$$

Reflection coefficients were calculated by normalising in-plane displacements (x-axis components) throughout the cracked plates due to the reflected wave against the amplitude of the incident S_0 wave (defined by Table 1) at identical positions in the cracked plates.

4 RESULTS

The reflection coefficient for the analysis of Fig. 2 is calculated by normalising the amplitude of the in-plane displacement against the amplitude of the incident wave, which is given in Table 2. The normalised amplitudes of the in-plane displacements have been calculated at different distances away from the crack at both the midplane and plate surface positions; the variation with time of those along the midplane some 5mm away from the crack are given in Fig. 3a. The normalised amplitude is seen to vary in an essentially sinusoidal manner (circular frequency, ω, = 10.0E6rads/sec). An initial transient phase is observed from $0 \leq$ time $\leq 16\mu$sec, and is caused by the initial stages of the reflected wave propagation. This is followed by a relatively long steady-state propagation phase. It is the maximum amplitude of the steady-state wave propagation that indicates the magnitude of the reflection coefficient, R. In this particular case, Fig. 3a, the reflection coefficient is some 14.2%. Such a value for a reflection coefficient is well above the signal noise levels that would be used with conventional digital signal processing techniques and it is therefore anticipated that this particular defect should be detectable in practice.

A further eight analyses have been performed in similar fashion. Crack lengths ranging from $0.4 \leq a/d \leq 0.6$ and three different frequencies were analysed. The reflection coefficients of these analysis are given in graphical form in Figs 3b-i and summarised in Table 3.

a/d	Ω = 0.534	Ω = 1.000	Ω = 1.600
0.4	0.0095	0.190	21.0
0.5	0.0165	0.373	25.5
0.6	0.028	0.740	14.2

Table 3: Reflection coefficients (units of %) predicted via finite element analyses for different horizontal defect lengths (2a) centrally embedded within aluminium plate (thickness 2d) given as a function of Rayleigh-Lamb dimensionless frequency, Ω.

There is a transient stage associated with each analysis, the duration of which varies with defect length and, to a lesser degree, frequency. Figure 4 presents the reflection coefficients for all nine analyses as a function of defect size and Rayleigh-Lamb wave frequency. It is clear that measurable reflection coefficients (>10%) can realistically only be obtained by using high frequency waves (Ω=1.6) since the magnitude of the reflection coefficients that would otherwise be measured (<1%) would be difficult to distinguish from the noise levels during digital signal processing.

The vibration and natural frequencies of undamaged composite plates and plates containing midplane delaminations were predicted recently by Tenek et al., [1993] using finite element methods. Negligible change in the first few natural frequencies (up to the 8th natural frequency) of plates containing even large delaminations was predicted. Higher order natural frequencies, however, were decreased and resonating delaminations dissipated mechanical energy into heat which was experimentally detected using vibrothermography and thermoelastic emission. Similar results were observed in the cracked plates of the present investigation. Natural frequencies were calculated for all the defects ($0.2 \leq a/d \leq 0.3$) via an eigenvalue analysis using two-dimensional finite element methods. The reduction of the first ten natural frequencies was not more than 0.2% of that of the corresponding natural frequencies of the uncracked plate. Natural frequencies up to 10^7 rads/sec were also obtained and the corresponding reduction was not more than 1%.

5 DISCUSSION

It is noteworthy to observe that the maximum amplitude of the reflected wave is not constant during the steady-state phase of the wave propagation, as shown typically in Fig. 3a, d and g. Some oscillation or degree of modulation of the wave is apparent. It is unclear at the present time whether this is due to numerical instability associated with the finite element analyses of the Ω=1.6 cases or to modulation of the reflected wave. However, the reflection coefficients have been taken as the average value of the maximum amplitude during the steady-state phase. A similar modulational instability was detected on finite gravity waves in deep water of arbitrary depth, h, (periodic wavetrains in nonlinear dispersive systems), which become unstable if the fundamental wavenumber k satisfies $kh > 1.363$. The greater the value of kh the more unstable the waves will be, in the sense that the modulational instability develops faster [Benjamin, 1967; Benjamin & Feir, 1967]. Future work will attempt to establish whether the instabilities in this system are due to physical phenomena or to numerical time stepping increments.

6 CONCLUSIONS

The propagation of Rayleigh-Lamb waves within thin aluminium plates has been examined and the reflection of such waves by symmetrically embedded cracks has been modelled in order to predict reflection coefficients. It has been predicted that measurable values of reflection coefficient (>10%) can be obtained by using high frequency waves (Ω=1.6). Future work being done by the author is aimed at determining the reflection coefficients of delaminations within composite plates; this will provide useful information on the lower bound limits to the use of Rayleigh-Lamb waves for NDE of composite structures.

ACKNOWLEDGEMENTS

The author is grateful to Professor L. J. Crane of Trinity College Dublin and the Institute for Numerical Computation and Analysis for developing the theoretical aspects of this paper and to Dr G. Thomas of University College Cork for identifying similar systems that exhibit physical instabilities. The author would like to thank University College Dublin for providing support in the form of a President's Research Award. This work constitutes part of the Brite-Euram SISCO project (Contract no. BRE2-CT94-0990).

REFERENCES

ABAQUS, 1996, Version 5.5. Hibbitt, Karlsson & Sorensen, Inc., RI, USA.

Al-Nassar, Y. N., Datta, S. K. & Shah, A. H., 1991, Scattering of Lamb waves by a normal rectangular strip weldment. *Ultrasonics*, 29, 125-31.

Benjamin, T. B., 1967, Instability of periodic wavetrains in nonlinear dispersive systems. *Proceedings of the Royal Society*, A**299**, 59-75.

Benjamin, T. B. & Feir, J. E., 1967, The disintegration of wave trains on deep water. *Journal of Fluid Mechanics*, **27**, (3), 417-30.

Bratton, R., Datta, S. K. & Shah, A. H., 1991, Scattering of Lamb waves in a composite plate. *Review of Progress in Quantitative NDE*, **10B**, 1507-14. D. O. Thompson & D. E. Chimenti, Eds., Plenum Press, New York.

Crane, L. J., Gilchrist, M. D. & Miller, J. J. H., 1997, Analysis of Rayleigh-Lamb wave scattering by a crack in an elastic plate. To appear in *Computational Mechanics.*

Datta, S. K., Shah, A. H. & Karunasena, W. M., 1990, Edge and layering effects in a multilayered composite plate. Computers & Structures, **37**, (2), 151-62.

Datta, S. K., Shah, A. H., Bratton, R. L. & Chakraborty, T., 1988, Wave propagation in laminated composite plates. *Journal of the Acoustical Society of America*, **83**, 2020-26.

Guo, N. & Cawley, P., 1993, The interaction of Lamb waves with delaminations in composite laminates. *Journal of the Acoustical Society of America*, **94**, (4), 2240-6

Guo, N. & Cawley, P., 1994, Lamb wave reflection for the quick nondestructive evaluation of large composite laminates. *Materials Evaluation*, March, 404-11.

Ju, T. H. & Datta, S. K., 1992, Pulse propagation in a laminated composite plate and nondestructive evaluation. *Comp. Eng.*, **2**, 55-66.

Karunasena, W. M., Shah, A. H. & Datta, S. K., 1991a, Plane-strain-wave scattering by cracks in laminated composite plates. *ASCE Journal of Engineering Mechanics*, **117**, 1738-54.

Karunasena, W. M., Shah, A. H. & Datta, S. K., 1991b, Reflection of plane strain waves at the free edge of a laminated composite plate. *Int. J. Solids & Structures*, **27**, (8), 949-64.

Koshiba, M., Karakida, S. & Suzuki, M., 1984, Finite-element analysis of Lamb wave scattering in an elastic plate waveguide. *IEEE Transactions on Sonics & Ultrasonics*, **SU-31**, (1), 18-24.

Rokhlin, S. I., 1979, Interaction of Lamb waves with elongated delaminations in thin sheets. *Int. Adv. in Nondestructive Testing*, **6**, 263-85.

Tenek, L. H., Henneke, E. G., II & Gunzburger, M. D., 1993, Vibration of delaminated composite plates and some applications to non-destructive testing. *Composite Structures*, **23**, 253-62.

Viktorov, I. A., 1967, *Rayleigh and Lamb Waves*. Plenum Press, New York.

Figure 1. Symmetric crack embedded in thin plate.

Figure 2. Finite element model of cracked plate. One quarter of the cracked plate is modelled availing of two planes of symmetry in the problem. Aspect ratio of this particular cracked plate is $a/d = 0.4$.

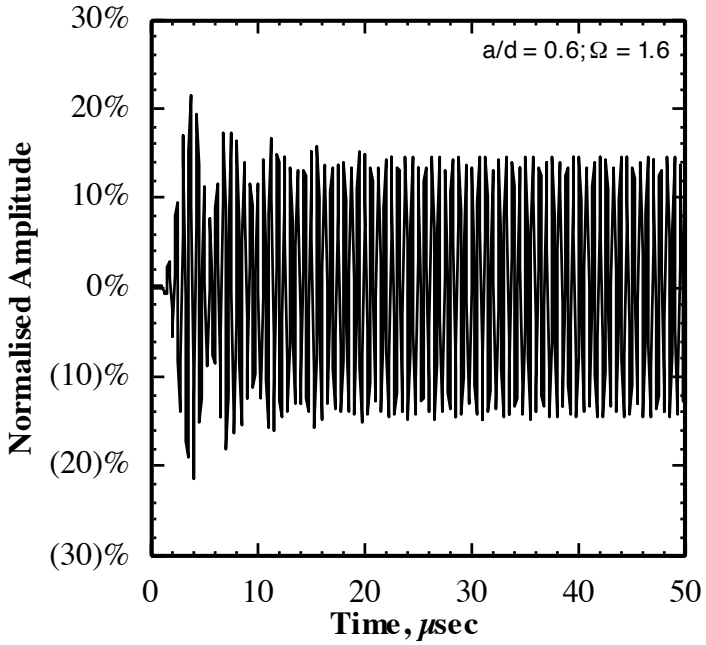

Figure 3a Normalised amplitude of the reflected wave calculated 5mm away from the end of the centrally embedded horizontal defect (a/d=0.6; Ω=1.6) at the midplane of the aluminium plate. The reflection coefficient is the magnitude of the normalised amplitude of the steady-state stage of the wave propagation (= 14.2% here).

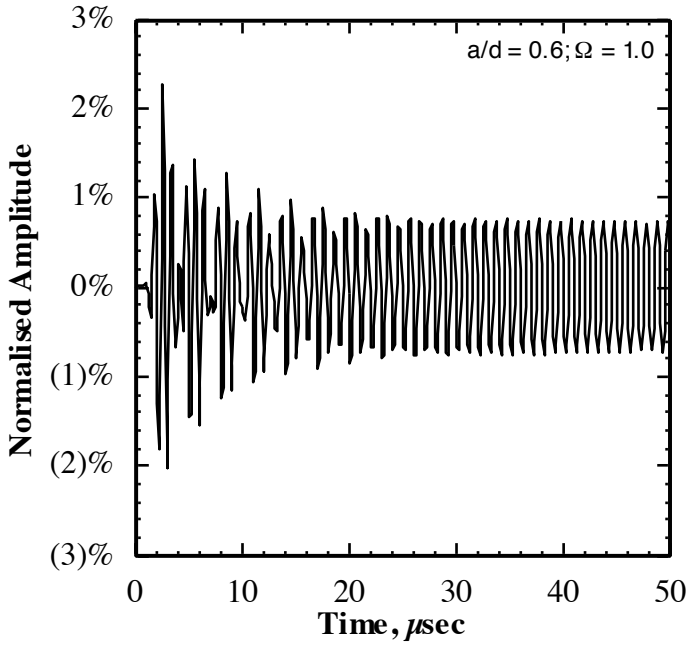

Figure 3b Normalised amplitude of the reflected wave calculated 5mm away from the end of the centrally embedded horizontal defect (a/d=0.6; Ω=1.0) at the midplane of the aluminium plate. The reflection coefficient is the magnitude of the normalised amplitude of the steady-state stage of the wave propagation (= 0.74% here).

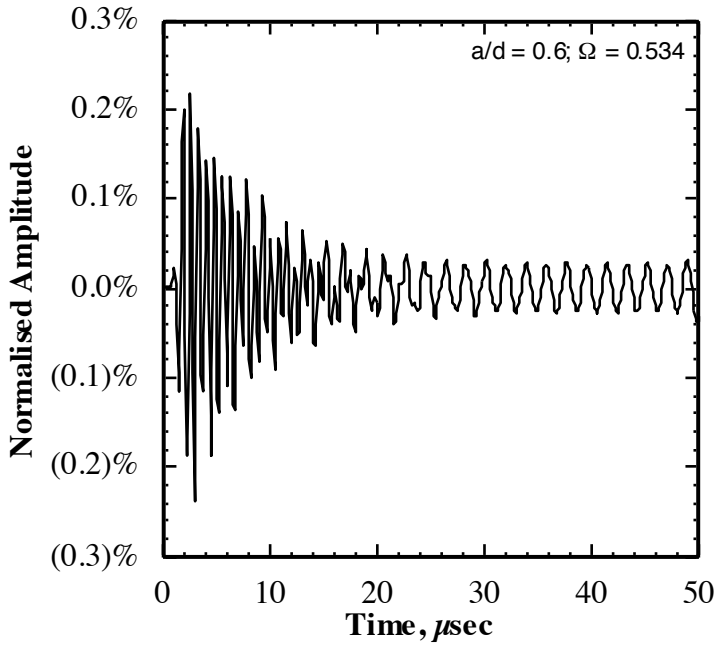

Figure 3c Normalised amplitude of the reflected wave calculated 5mm away from the end of the centrally embedded horizontal defect (a/d=0.6; Ω=0.534) at the midplane of the aluminium plate. The reflection coefficient is the magnitude of the normalised amplitude of the steady-state stage of the wave propagation (= 0.028% here).

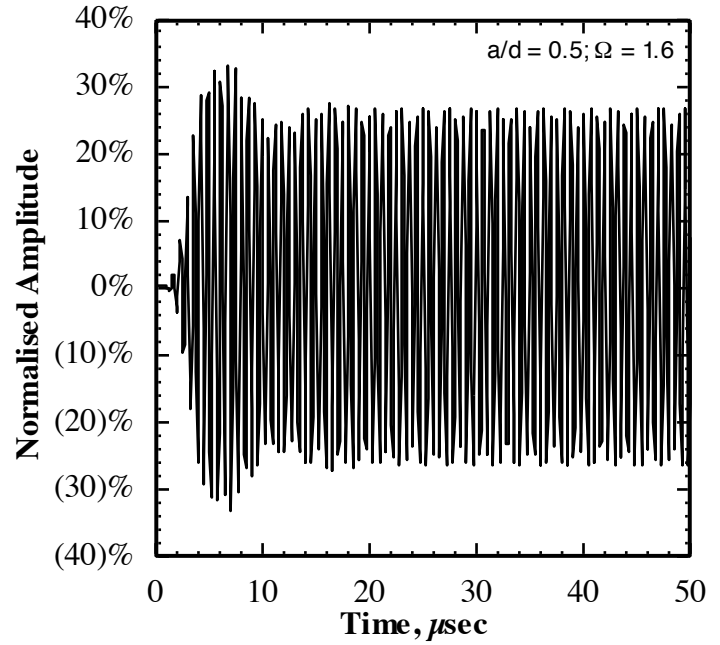

Figure 3d Normalised amplitude of the reflected wave calculated 5mm away from the end of the centrally embedded horizontal defect (a/d=0.5; Ω=1.6) at the midplane of the aluminium plate. The reflection coefficient is the magnitude

of the normalised amplitude of the steady-state stage of the wave propagation (= 25.5% here).

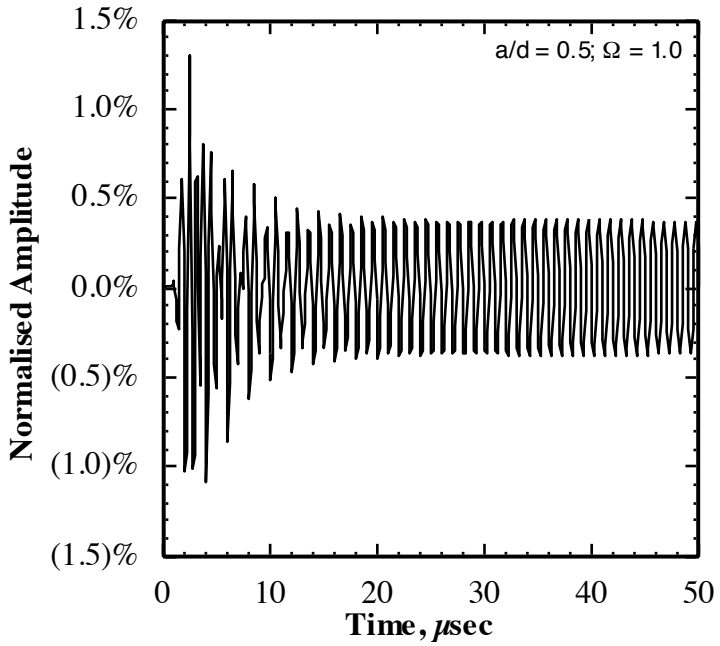

Figure 3e Normalised amplitude of the reflected wave calculated 5mm away from the end of the centrally embedded horizontal defect (a/d=0.5; Ω=1.0) at the midplane of the aluminium plate. The reflection coefficient is the magnitude of the normalised amplitude of the steady-state stage of the wave propagation (= 0.373% here).

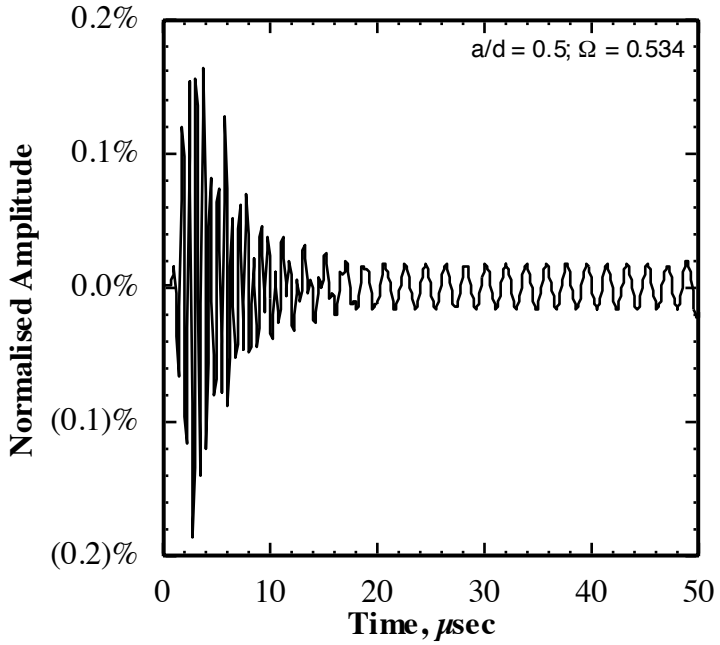

Figure 3f Normalised amplitude of the reflected wave calculated 5mm away from the end of the centrally embedded horizontal defect (a/d=0.5; Ω=0.534) at the

midplane of the aluminium plate. The reflection coefficient is the magnitude of the normalised amplitude of the steady-state stage of the wave propagation (= 0.0165% here).

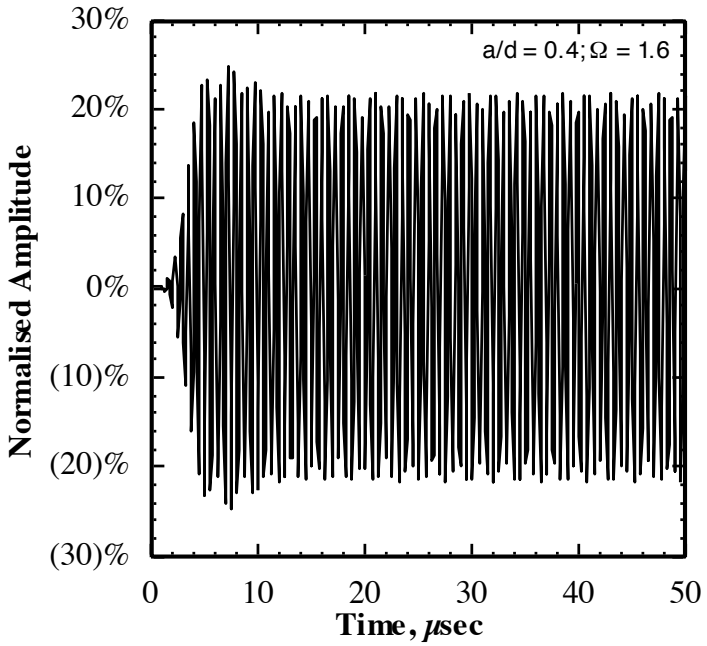

Figure 3g Normalised amplitude of the reflected wave calculated 5mm away from the end of the centrally embedded horizontal defect (a/d=0.4; Ω=1.6) at the midplane of the aluminium plate. The reflection coefficient is the magnitude of the normalised amplitude of the steady-state stage of the wave propagation (= 21.0% here).

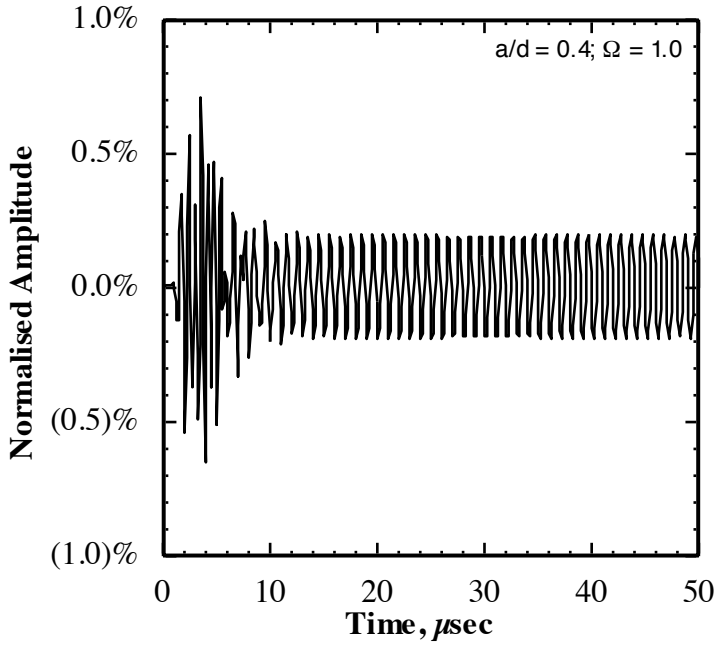

Figure 3h Normalised amplitude of the reflected wave calculated 5mm away from the end of the centrally embedded horizontal defect (a/d=0.4; Ω=1.0) at the

midplane of the aluminium plate. The reflection coefficient is the magnitude of the normalised amplitude of the steady-state stage of the wave propagation (= 0.19% here).

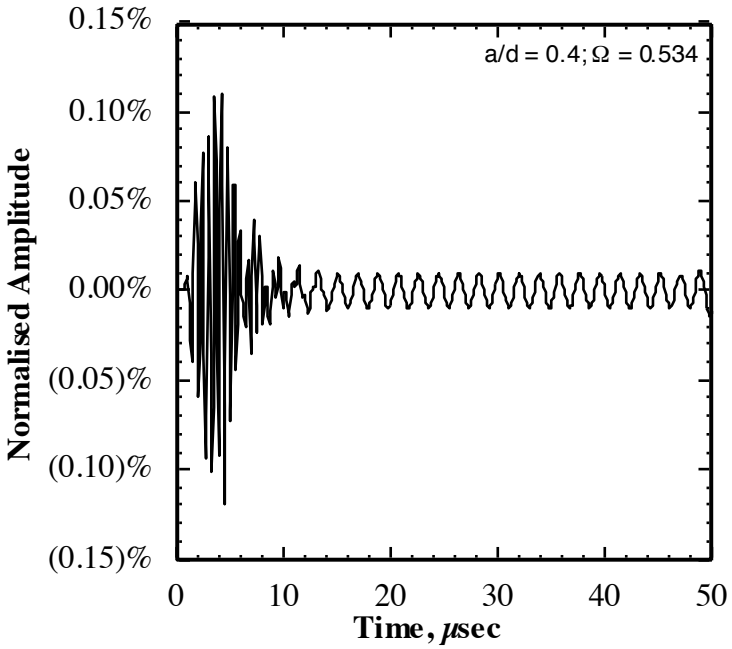

Figure 3i Normalised amplitude of the reflected wave calculated 5mm away from the end of the centrally embedded horizontal defect (a/d=0.4; Ω=0.534) at the midplane of the aluminium plate. The reflection coefficient is the magnitude of the normalised amplitude of the steady-state stage of the wave propagation (= 0.0095% here).

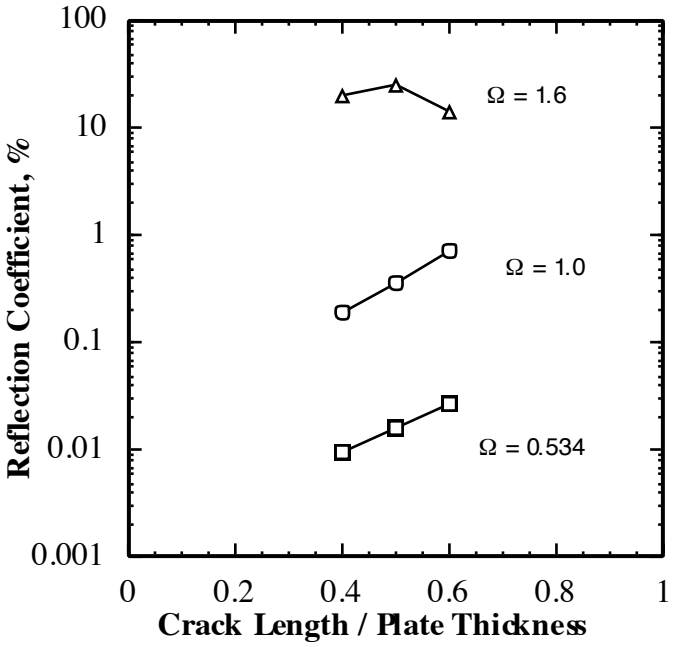

Figure 4 Summary of reflection coefficients for defects of size $a/d \leq 0.4 \leq 0.6$ and incident S_0 Rayleigh-Lamb waves of three different frequencies, Ω. Summarised from the results of Fig. 3.